

This is an Open Access document downloaded from ORCA, Cardiff University's institutional repository:<https://orca.cardiff.ac.uk/id/eprint/124924/>

This is the author's version of a work that was submitted to / accepted for publication.

Citation for final published version:

Ratcliff, Michael, Rees, Daniel, McGrady, Scott, Buntwal, Luke, Hornsby, Amanda K. E., Bayliss, Jaqueline, Kent, Brianne A., Bussey, Timothy, Saksida, Lisa, Beynon, Amy L., Howell, Owain W., Morgan, Alwena H., Sun, Yuxiang, Andrews, Zane B., Wells, Timothy and Davies, Jeffrey S. 2019. Calorie restriction activates new adult born olfactory-bulb neurones in a ghrelin-dependent manner but acyl-ghrelin does not enhance subventricular zone neurogenesis. *Journal of Neuroendocrinology* 31 (7) , -. 10.1111/jne.12755

Publishers page: <http://dx.doi.org/10.1111/jne.12755>

Please note:

Changes made as a result of publishing processes such as copy-editing, formatting and page numbers may not be reflected in this version. For the definitive version of this publication, please refer to the published source. You are advised to consult the publisher's version if you wish to cite this paper.

This version is being made available in accordance with publisher policies. See <http://orca.cf.ac.uk/policies.html> for usage policies. Copyright and moral rights for publications made available in ORCA are retained by the copyright holders.



1 **Calorie restriction activates new adult born olfactory-bulb neurones in**  
2 **a ghrelin-dependent manner but acyl-ghrelin does not enhance sub-**  
3 **ventricular zone neurogenesis**

4 Michael Ratcliff<sup>1</sup>, Daniel Rees<sup>1\*</sup>, Scott McGrady<sup>1</sup>, Luke Buntwal<sup>1</sup>, Amanda K. E. Hornsby<sup>1</sup>, Jaqueline  
5 Bayliss<sup>2</sup>, Brianne A. Kent<sup>3</sup>, Timothy Bussey<sup>4</sup>, Lisa Saksida<sup>4</sup>, Amy L Beynon<sup>1</sup>, Owain W Howell<sup>1</sup>,  
6 Alwena H. Morgan<sup>1</sup>, Y Sun<sup>5</sup>, Zane B. Andrews<sup>2</sup>, Timothy Wells<sup>6</sup>, Jeffrey S. Davies<sup>1§</sup>

7

8 <sup>1</sup>Molecular Neurobiology, Institute of Life Sciences, School of Medicine, Swansea University, UK.  
9 SA28PP. <sup>2</sup>Department of Physiology, Biomedical Discovery Unit, Monash University, Melbourne,  
10 Australia. <sup>3</sup>Department of Medicine, Vancouver, University of British Columbia, Canada. <sup>4</sup>Western  
11 University, London, Ontario, Canada. <sup>5</sup>Department of Nutrition and Food Science, Texas A&M  
12 University, College Station, USA. <sup>6</sup>School of Biosciences, Cardiff University, UK.

13 §Correspondence should be addressed to [jeff.s.davies@swansea.ac.uk](mailto:jeff.s.davies@swansea.ac.uk)

14 \*Current address: School of Management, Swansea University, Bay Campus, Swansea, SA1 8EN,  
15 UK

16 Keywords: Ghrelin, Neurogenesis, Olfactory bulb, Sub-ventricular zone, Calorie restriction

17

18 Figures: 4

19 Supplementary figures: 5

20 Highlights

- 21 • Acyl-ghrelin receptor, GHSR, is not expressed in the SVZ
- 22 • Acyl-ghrelin does not modulate SVZ cell proliferation
- 23 • Acyl-ghrelin does not increase adult olfactory bulb neurogenesis
- 24 • Genetic ablation of ghrelin does not affect survival of new adult born neurones
- 25 • Acyl-ghrelin receptor, GHSR, is expressed in the olfactory bulb
- 26 • Calorie restriction activates new adult born neurones in a ghrelin-dependent manner

27

28

29 Dr Jeffrey S Davies,  
30 Molecular Neurobiology,  
31 Institute of Life Sciences,  
32 School of Medicine,  
33 Swansea University,  
34 UK. SA2 8PP.

35

36 Tel: +44 (0)1792 602209

37 [jeff.s.davies@swansea.ac.uk](mailto:jeff.s.davies@swansea.ac.uk)

38 **Abstract**

39 The ageing and degenerating brain show deficits in neural stem/progenitor cell (NSPC) plasticity  
40 that are accompanied by impairments in olfactory discrimination. Emerging evidence suggests  
41 that the gut-hormone ghrelin plays an important role in protecting neurones, promoting synaptic  
42 plasticity and increasing hippocampal neurogenesis in the adult brain. Here, we studied the role  
43 of ghrelin in modulating adult sub-ventricular zone (SVZ) NSPCs that give rise to new olfactory  
44 bulb (OB) neurones. We characterised the expression of the ghrelin receptor, growth hormone  
45 secretagogue receptor (GHSR), using an immuno-histochemical approach in GHSR-eGFP reporter  
46 mice to show that GHSR is expressed in several regions, including the OB, but not in the SVZ of  
47 the lateral ventricle. These data suggest that acyl-ghrelin does not mediate a direct effect on NSPC  
48 in the SVZ. Consistent with these findings, treatment with acyl-ghrelin or genetic silencing of  
49 GHSR did not alter NSPC proliferation within the SVZ. Similarly, using a BrdU pulse-chase  
50 approach we show that peripheral treatment of adult rats with acyl-ghrelin did not increase the  
51 number of new adult-born neurones in the granule cell layer (GCL) of the OB. These data  
52 demonstrate that acyl-ghrelin does not increase adult OB neurogenesis. Finally, we studied  
53 whether elevating ghrelin indirectly, via calorie restriction (CR), regulated the activity of new  
54 adult-born cells in the OB. Overnight CR induced c-Fos expression in new adult-born OB cells, but  
55 not in developmentally born cells, whilst neuronal activity was lost following re-feeding. These  
56 effects were absent in ghrelin<sup>-/-</sup> mice, suggesting that adult-born cells are uniquely sensitive to  
57 changes in ghrelin mediated by fasting and re-feeding. In summary, ghrelin does not promote  
58 neurogenesis in the SVZ and OB, however, new adult-born OB cells are activated by CR in a  
59 ghrelin-dependent manner.

60

61

62

63

## 64 **Introduction**

65 The generation of new adult-born neurones in the olfactory bulb (OB) continues throughout life  
66 and contributes to olfactory memory. The adult OB receives new neurones that originate from  
67 divided neural stem / progenitor cells (NSPCs) residing in the sub-ventricular zone (SVZ)  
68 adjacent to the lateral ventricles. Following NSPC division, the cells differentiate into immature  
69 neuroblasts and migrate along the rostral migratory stream (RMS) prior to integration with local  
70 OB circuitry<sup>1</sup>. This process of adult OB neurogenesis (AOBN) is regulated by several intrinsic and  
71 extrinsic factors including age, exercise, inflammation and glucocorticoids<sup>1</sup>. However, the  
72 underlying mechanisms mediating this process are poorly understood.

73

74 Within the OB, new adult-born neurones promote olfactory memory and enhance the ability to  
75 discriminate distinct odours<sup>2,3</sup>. AOBN is also important for OB granule cell replacement and tissue  
76 maintenance<sup>4</sup>. Olfactory impairment has been reported as a prodromal indicator of several  
77 neurodegenerative diseases<sup>5</sup>. For example, deficits in olfactory discrimination (i.e the ability to  
78 distinguish odours) have been described in experimental neurodegenerative animal models and  
79 human Parkinson's disease<sup>6</sup>.

80

81 Ghrelin, an orexigenic gut hormone produced in response to calorie restriction, acts on the  
82 hypothalamus to stimulate the release of growth hormone (GH), and promote meal initiation and  
83 food intake. Emerging evidence suggests that acyl-ghrelin may also have important extra-  
84 hypothalamic functions<sup>7</sup>, such as increasing olfactory sensitivity<sup>8</sup> and regulating activity in brain  
85 regions involved in olfaction and appetitive behaviour<sup>9</sup>.

86 In the neurogenic niche of the hippocampus, acyl-ghrelin has been shown to increase cell  
87 proliferation<sup>10</sup> and the number of new adult-born neurones in adult rodents<sup>11</sup>. The ghrelin  
88 receptor, GHSR, which is expressed within the dentate gyrus of the hippocampus, mediates the  
89 pro-neurogenic effect of calorie restriction (CR)<sup>12</sup>, as well as the increase in hippocampal  
90 neurogenesis and antidepressant-like effect following P7C3 treatment<sup>13</sup>. Moreover, ghrelin  
91 deficient mice are reported to have impaired cell proliferation in the SVZ that is normalised to  
92 wild-type levels with exogenous acyl-ghrelin treatment<sup>14</sup>. GHSR is the only molecularly identified  
93 receptor for ghrelin, mediating the central effects of this hormone on appetite, body weight and  
94 energy metabolism<sup>15</sup>. However, it is not known whether GHSR is expressed within the neurogenic  
95 niche of the SVZ or whether acyl-ghrelin modulates adult olfactory bulb neurogenesis (AOBN).  
96 Here, we aimed to determine the expression pattern of GHSR within the SVZ and whether ghrelin  
97 modulates AOBN.

98 In addition, as fasting and feeding increase<sup>16</sup> and decrease olfactory sensitivity<sup>17</sup>, respectively, we  
99 sought to determine whether ghrelin modulates the fasting-induced activation of both new adult-  
100 born and developmentally-born OB neurones.

101 **Materials and Methods**

102

103 **Animals and procedures**

104 All experiments involving animals were performed with appropriate ethical approval. Mouse  
105 studies were performed at Cardiff University (GHSR-null, Ghrelin<sup>-/-</sup>) and Monash University  
106 (GHSR-eGFP). Studies involving rats were performed at the University of Cambridge.

107

108 **Mice**

109 ***GHSR-eGFP mice***: Adult male GHSR-eGFP reporter mice were housed at room  
110 temperature on a 12h light, 12h dark cycle (0700-1900h) with free access (*ad libitum*) to  
111 food and water. GHSR-eGFP reporter mice<sup>18</sup> (n=6) were obtained from the Mouse Mutant  
112 Regional Resource Center at the University of California Davis, and the hemizygous mice  
113 back-crossed to C57BL/6J mice. GHSR-eGFP reporter mice were terminally anaesthetised  
114 and trans-cardially perfused with 4% paraformaldehyde (PFA) in 0.1M PBS. Whole brains  
115 were rapidly removed and post-fixed in ice cold 4% PFA for 24h at 4°C before being sunk  
116 in 30% sucrose. Finally, brains were transferred to PBS + 0.1% sodium azide (Sigma  
117 Aldrich, St Louis, USA) and stored at 4°C prior to analysis. Brains were frozen using a fine  
118 powder of ground-up dry ice and mounted on a sliding sledge freezing microtome (Zeiss,  
119 Microm HM 450) using Jung's freezing medium. The thermostat was set to -30°C to  
120 ensure brains remained frozen. 30µm thick coronal sections cut along the entire rostral-  
121 caudal axis (bregma +5.345mm to -4.08) were collected in a 96-well plate (Nunc, nunclon  
122 surface) filled with PBS + 0.1% sodium azide and stored at 4°C until required. Ghsr-eGFP  
123 mouse brains were also collected in a sagittal orientation (bregma +3.925 to -0.20).

124 ***Immunofluorescence for GHSR-GFP***: All experiments were performed on free-floating tissue  
125 sections at room temperature, unless stated otherwise. A 1 in 6 series of coronal or sagittal brain  
126 sections were selected (minimum of 10 sections per mouse), transferred into a 24-well culture  
127 plate (Nunc, nunclon surface) and washed in PBS (Sigma Aldrich, St Louis, USA) three times for 5  
128 minutes each. Tissue sections were then permeabilised in methanol (Fisher Scientific,  
129 Loughborough, UK) at -20°C for 2 minutes and washed (as before) in PBS. Non-specific binding  
130 sites were blocked with 5% normal goat serum (NGS) (Sigma Aldrich, St Louis, USA) in PBS +  
131 0.1% triton x-100 (Sigma Aldrich, Gillingham, UK) (PBS-T) for 1h. Excess block was removed and  
132 tissue sections incubated with chicken anti-GFP (Chicken polyclonal, Abcam, Cambridge, UK,  
133 Ab13970), diluted 1:1000 in PBS-T, for 24h at 4°C. Primary antibody was omitted from the

134 negative control. Sections were washed and incubated in goat anti-chicken Alexa-fluor 488 (Goat  
135 polyclonal, Life technologies, USA, A11039), diluted 1:500 in PBS-T, for 30 minutes in the dark.  
136 Finally, sections were washed, mounted onto Superfrost<sup>+</sup> slides (Fisherbrand, Superfrost<sup>+</sup> slides)  
137 and cover-slipped with vectashield (containing DAPI) (Vector Labs, Burlingame, USA) before  
138 being stored at 4°C. The slides were analysed by laser scanning confocal microscopy (Zeiss,  
139 LSM710) and Zen software (Zeiss, Zen 2010 edition) after 24h. Freely available GIMP v2.8  
140 software was used to prepare tiled images of coronal and sagittal sections ([www.gimp.org](http://www.gimp.org)).

141 **GHSR-null mice:** For assessing exogenous acyl-ghrelin regulation of SVZ cell proliferation,  
142 homozygous male loxTB-GHSR mice (GHSR-null) (a gift from Prof Jeffrey Zigman, University of  
143 Texas Southwestern Medical Center, Dallas, TX) and W-T (C57BL/6J; W-T) controls (Harlan UK  
144 Ltd.) (14 weeks-old, n = 3 / group) were used<sup>19</sup>. The methodological and metabolic aspects of this  
145 study have previously been described<sup>20</sup>. Briefly, mice were prepared with jugular vein cannulae  
146 attached to osmotic mini-pumps (Alzet model 2001) under isoflurane anesthesia. The mini-  
147 pumps delivered either vehicle or acyl-ghrelin (48µg/day; Phoenix Pharmaceuticals, USA) for 7  
148 days. This treatment protocol was shown to increase abdominal adiposity via GHSR, but had no  
149 effect on body weight<sup>20</sup>. Mice were euthanised by cervical dislocation and whole trunk blood was  
150 collected into heparinized tubes for plasma separation by centrifugation at 4,000g for 10 minutes  
151 at 4°C. Whole brain was removed and immediately snap frozen on dry ice and stored at -80°C  
152 prior to analysis.

153 For analysis of Ki67, snap-frozen brains were sectioned at 10µm thickness using a cryostat  
154 (Leica) and mounted directly onto superfrost<sup>+</sup> coated slides (VWR). A one-in-fifteen series of  
155 10µm sections (150µm apart) from each animal, a minimum of 8 sections per mouse, was  
156 immunostained using rabbit anti-Ki67 (1:500, ab16667, Abcam) along with a biotinylated goat  
157 anti-rabbit for Ni-DAB based detection, as previously described<sup>11</sup>. Cells were imaged by light  
158 microscopy (Nikon 50i) prior to quantification using Image J software.

159 A separate cohort of 19-week old male GHSR-null mice, derived from crosses between animals  
160 that were heterozygous for the GHSR-null allele and that had been backcrossed >10 generations  
161 onto a C57BL/6J genetic background, and WT littermate mice were housed under normal  
162 laboratory conditions (12 h light: 12 h dark, lights on at 06.00 h) (n=3/genotype). Mice were  
163 killed by cervical dislocation under terminal anaesthesia, whole brain was removed, immersed in  
164 4% PFA for 24h at 4°C and cryoprotected in 30% sucrose prior to preparation of coronal sections  
165 (30µm) cut into a 1:12 series along the entire rostro-caudal extent of the brain using a freezing-  
166 stage microtome (MicroM, ThermoScientific) and collected for IHC. For DAB-

167 immunohistochemical analysis of GHSR labelling, a minimum of 6 sections per mouse were  
168 washed in 0.1M PBS (2× 10min) and 0.1M PBS-T (1× 10min). Subsequently, endogenous  
169 peroxidases were quenched by washing in a PBS plus 1.5% H<sub>2</sub>O<sub>2</sub> solution for 20min. Sections  
170 were washed again (as above) and incubated in 5% NDS in PBS-T for 1h. Sections were incubated  
171 overnight at 4°C with rabbit anti-GHSR1a (Phoenix Pharmaceuticals, H-001-62), diluted 1:2000  
172 in PBS-T and 2% NGS solution. Another wash step followed prior to incubation with biotinylated  
173 goat anti-rabbit (1:400; Vectorlabs, USA) in PBS-T for 70min. The sections were washed and  
174 incubated in ABC (Vector- labs, USA) solution for 90min in the dark prior to another two washes  
175 in PBS, and incubation with 0.1 M sodium acetate pH6 for 10min. Immunoreactivity was  
176 developed in Nickel enhanced DAB solution followed by two washes in PBS. Sections were  
177 mounted onto superfrost<sup>+</sup> slides (VWR, France) and allowed to dry overnight before being de-  
178 hydrated and de-lipified in increasing concentrations of ethanol. Finally, sections were incubated  
179 in histoclear (2× 3min; National Diagnostics, USA) and coverslipped using entellan mounting  
180 medium (Merck, USA). Slides were allowed to dry overnight prior to imaging.

181 **Calorie restriction in Ghrelin<sup>-/-</sup> mice:** Adult female homozygous ghrelin knockout (ghrelin<sup>-/-</sup>)  
182 mice<sup>21</sup> and their wild type (WT) littermates were derived from crosses between animals that  
183 were heterozygous for the ghrelin-null allele. These mice were backcrossed >10 generations on  
184 a C57BL/6J genetic background and acclimatized to being individually housed for 7 days under  
185 normal laboratory conditions (12h light, 12h dark cycle; 0700-1900h) prior to the onset of the  
186 study. Mice were divided into six groups (n=5-8/group) that included *ad-libitum* fed WT, calorie  
187 restricted (CR) WT, calorie restricted/re-fed (CR/RF) WT, *ad-libitum* fed ghrelin<sup>-/-</sup>, CR ghrelin<sup>-/-</sup>  
188 and CR/RF ghrelin<sup>-/-</sup>. For the first 28 days of the study, mice were fed on an *ad-libitum* diet with  
189 daily injections (from days 1-4) of the thymidine analogue, BrdU (50mg/kg; i.p), to label actively  
190 dividing cells. On day 28, food was withdrawn at 17.30h from the CR and CR/RF mice. On the  
191 subsequent day, CR/RF mice were allowed to feed *ad-libitum* for 1h prior to all animals  
192 undergoing cervical dislocation whilst under terminal anaesthesia (~18h CR). Ghrelin<sup>-/-</sup> mice  
193 have growth rates and appetite similar to WT littermates, with no impairment in hyperphagia  
194 after fasting<sup>21,22</sup>. Similarly, adult ablation of ghrelin in mice does not impair growth nor appetite<sup>23</sup>.  
195 Whole brains were removed, immersed in ice cold 4% PFA for 24h and cryoprotected in 30%  
196 sucrose. Coronal sections (30µm) were cut in a 1:12 series along the entire rostral-caudal axis of  
197 the olfactory bulb (bregma +5.345mm to +2.445mm) using a freezing stage microtome (MicroM,  
198 Thermo Scientific) and collected for IHC.

199

200 **Quantification of BrdU<sup>+</sup>/c-Fos<sup>+</sup>:** All IHC was performed on free-floating sections at room  
201 temperature, unless otherwise stated. A 1:6 series of 30µm sections (180µm apart) were washed



202 three times in PBS for 5 min, permeabilised in methanol at -20°C for 2 min, and washed as before.  
203 DNA was denatured with 2M HCL for 30 min at 37°C prior to washing sections in 0.1M borate  
204 buffer (pH 8.5) for 10 minutes. Sections were washed, blocked with 5% normal goat serum (NGS)  
205 plus 5% bovine serum albumin (BSA) in PBS plus 0.1% Triton (PBS-T) for 60 min and incubated  
206 in a cocktail of primary antibodies that included rat anti-BrdU (1:400; MCA2060, ABD Serotec)  
207 and rabbit anti-c-Fos (1:1000; SC-52, Santa Cruz) in PBS-T overnight at 4°C. The primary antibody  
208 was omitted from the negative control.

209 Following primary antibody treatment, sections were washed, incubated with biotinylated goat  
210 anti-rat (1:400; BA-9400, Vector Labs) in PBS-T for 60 min in the dark and then washed as before.  
211 Similarly, secondary antibodies were also applied as a cocktail that included goat anti-rabbit  
212 (1:400; BA-1000, Vector Labs) and streptavidin AF-594 (1:500; S11227, Life Technologies) in  
213 PBS-T for 30 min. Following another wash, including one containing Hoechst nuclear stain,  
214 sections were mounted onto superfrost+ slides (VWR, France) and cover-slipped with prolong  
215 gold anti-fade solution (Life Technologies, USA).

216

217 **Quantification of immunolabelled cells:** A 1:6 series of 30µm sections (180µm apart) from each  
218 animal was analysed for immunoreactivity using an epi-fluorescent microscope system (Zeiss,  
219 Imager M1 with Axiocam MRm). Immunolabelled cells were manually counted bilaterally using a  
220 ×40 objective through the z-axis of the entire rostral-caudal extent of the dorsal granule cell layer  
221 (GCL), glomerular layer (GL), subependymal zone (SEZ) and the lateral olfactory tract body (LOT).  
222 Resulting numbers were divided by the total area measurement to give a count per pixel, which  
223 was converted into mm<sup>2</sup> and averaged for each brain. All analyses were performed blind to both  
224 genotype and treatment.

225

## 226 **Rats**

227 Adult male lister hooded rats (n=10/11 per group, weighing 250-300g; Harlan, Bicester, UK)  
228 were housed in groups of four and maintained at room temperature on a 12h light, 12h dark cycle  
229 (0700-1900h). These experimental procedures have previously been described<sup>11</sup>. Briefly, from  
230 days 0-14, rats received daily intra-peritoneal injections of acyl-ghrelin (Phoenix  
231 Pharmaceuticals, 031-31) or saline (10µg/kg body weight) with BrdU injections (50mg/kg) on  
232 days 5-8. On day 29, rats were terminally anaesthetised, trans-cardially perfused with 4% PFA  
233 and brains were removed for immersion fixation and cryoprotection (as before). Analysis of adult  
234 hippocampal neurogenesis (AHN) in these rats demonstrated that acyl-ghrelin significantly  
235 increased the number of new adult born neurones<sup>11</sup>.

236

237 **Double immunofluorescence for BrdU/NeuN:** A 1 in 6 series of coronal OB brain sections  
238 (bregma +5.345mm to +2.445) were transferred into a 24-well culture plate and washed in PBS,  
239 permeabilised in methanol at -20°C for 2 minutes and washed in PBS as before. DNA was  
240 denatured using 2M hydrochloric acid (HCL) (Fisher Scientific, Loughborough, UK) and incubated  
241 at 37°C for 30 minutes. Excess HCL was removed and the sections washed in 0.1M borate buffer,  
242 pH 8.5, for 10 minutes to neutralise the remaining HCL. Tissue sections were then washed,  
243 blocked with 5% NGS diluted in PBS-T for 1h and incubated with rat anti-BrdU (Rat monoclonal,  
244 ABD Serotec, Oxfordshire, UK, MCA2060), diluted 1:3000 in PBS-T for 24h at 4°C. The primary  
245 antibody was omitted from the negative control. Sections were washed and incubated with  
246 biotinylated goat anti-rat (Goat polyclonal, Vector labs, Burlingham, USA, BA-9400), diluted 1:400  
247 in PBS-T for 1h in the dark. Tissue sections were subsequently washed, incubated in streptavidin  
248 AF594 (Life technologies, Eugene, USA, S11227), diluted 1:500 in PBS-T for 30 minutes and  
249 washed as before. Sections were then incubated in mouse anti-NeuN (Mouse monoclonal, EMD  
250 Millipore, Massachusetts, USA, MAB377), diluted 1:1000 in PBS-T for 1h. The negative control  
251 contained PBS-T. Tissue sections were then washed and incubated in goat anti-mouse AF 488  
252 diluted 1:500 in PBS-T for 30 minutes, prior to being washed with Hoescht, diluted 1:10000 in  
253 PBS, for 5 minutes. Finally, sections were washed, mounted onto Superfrost+ slides and cover-  
254 slipped with prolong gold anti-fade reagent, prior to storage at 4°C.

255

256 **Quantification of BrdU<sup>+</sup>:** Image J software (version 1.47) was used to quantify the number of new  
257 adult-born cells in the dorsal and ventral granular cell layer (GCL) of the OB. Images taken by the  
258 fluorescent microscope were inverted and unsharp-masked, using a radius of 10.0 pixels and a  
259 mask weight of 0.60. The polygon tool was then used to draw around the granular cell layer and  
260 the total area measured. Each image's threshold was individually optimised, typically ranging  
261 from 0.100 – 0.180. The particle size was set to 20-300 pixel<sup>2</sup> and circularity at 0.0-1.0. Resulting  
262 numbers were divided by the total area measurement to give a count per pixel, which was then  
263 averaged for each brain.

264

265 **Quantification of BrdU<sup>+</sup>/NeuN<sup>+</sup>:** To quantify the number of new adult-born neurons in the dorsal  
266 and ventral granular cell layer of the OB, BrdU<sup>+</sup>/NeuN<sup>+</sup> immunoreactive cells were manually  
267 counted through the z-axis of the entire rostral-caudal extent of the OB. Resulting numbers were  
268 divided by the area of the z-stack to give a count per pixel, which was then averaged for each  
269 brain.

270

271 **Microscopy**

272 Tissue sections were analysed using a fluorescent microscope (Zeiss, Imager M1 with AxioCam  
273 MRm) with Axiovision software (version 4.6) and a laser scanning confocal microscope (Zeiss,  
274 LSM 710) with Zen software (Zen 2010 edition). Images were collected using  $\times 4$ ,  $\times 10$  and  $\times 40$   
275 objectives. BrdU<sup>+</sup>/NeuN<sup>+</sup> immunoreactive newborn adult neurones, in the dorsal and ventral GCL,  
276 were imaged using a  $\times 40$  oil immersion objective. A z-stack consisting of 21-25 tissue slices at  
277  $0.7\mu\text{m}$  intervals ( $14.0\text{-}16.8\mu\text{m}$  range) were taken throughout the rostral-caudal extent of the OB.  
278 All experiments and analyses were performed blind to genotype and treatment.

279

280 **Statistical Analysis**

281 Statistical analyses were performed using GraphPad Prism 6.0 for Mac (GraphPad Software, San  
282 Diego, CA). Statistical significance was assessed by an unpaired two-tailed Student's *t*-test or one-  
283 way ANOVA with Bonferroni's *post-hoc* test. Where there was more than one variable a two-way  
284 ANOVA with Tukey's multiple comparisons test was used or a Kruskal-Wallis test followed by a  
285 Dunn's multiple comparisons test was used when a normal distribution of data could not be  
286 assumed. Data are presented as a mean  $\pm$ SEM. \*,  $P<0.05$ ; \*\*,  $P<0.01$ ; \*\*\*,  $P<0.001$  and \*\*\*\*,  
287  $P<0.0001$  were considered statistically significant.

288

289

290 **Results**

291 **GHSR is expressed in the adult OB but not in the SVZ**

292 The expression of GHSR was assessed to determine whether ghrelin could directly influence the  
293 proliferation of NSPCs in the SVZ. To achieve this aim we used GHSR-eGFP reporter mice to show  
294 that eGFP immunoreactivity was present within the anterior olfactory nucleus (AON) and orbital  
295 and motor orbital cortex in the caudal OB (figure 1i). Immunoreactivity was observed within the  
296 anterior cingulate cortex, motor cortex and lateral septal nucleus (figure 1ii). Sagittal sections  
297 revealed strong immunoreactivity in the anterior amygdala area, granule cell layer of the  
298 hippocampal dentate gyrus (DG) and the medial amygdala nucleus (figure 1iii). Notably, staining  
299 was absent within the lateral lining of the SVZ in tissue sectioned in both a coronal and sagittal  
300 orientation (figure 1iiD and iiiC). To determine whether the GHSR-eGFP immunoreactivity was  
301 similar to that observed with GHSR1a antisera, we performed IHC using a rabbit anti-GHSR1a  
302 antibody on adult WT and GHSR-null mouse brain tissue. These analyses revealed a similar  
303 pattern of immunoreactivity on both WT and GHSR-null tissues, including the SVZ (figure S1),  
304 suggesting a lack of binding specificity for the GHSR1a antigen. These data suggest that ghrelin  
305 may be involved in olfactory function but not through direct modulation of NSC's lining the lateral  
306 wall of the SVZ.

307

308 **Acyl-ghrelin does not increase cell proliferation in the adult SVZ**

309 The proliferative effect of ghrelin and GHSR-agonists have been widely reported within CNS and  
310 peripheral tissues<sup>24-26</sup>. A recent study reported that ghrelin promoted proliferation of cells within  
311 the SVZ<sup>14</sup>. Here, we took advantage of genetically modified mice to analyse the effect of acyl-  
312 ghrelin treatment on SVZ cell proliferation in adult WT and GHSR-null mice, where GHSR is  
313 transcriptionally silenced. Using the mitotic marker, Ki67, we report that acyl-ghrelin treatment  
314 had no effect on the number of proliferating cells within the SVZ niche in WT mice (figure 2,  $P =$   
315  $>0.99$ ). Similarly, transcriptional silencing of GHSR did not affect the rate of SVZ cell division in  
316 vehicle (WT veh vs GHSR-null veh,  $P = 0.6388$ ) or acyl-ghrelin treated mice (GHSR-null veh vs  
317 GHSR-null acyl-ghrelin,  $P = 0.0944$ ). The low number of replicates means that the statistical  
318 analysis is of low power, however, the data suggest that acyl-ghrelin does not regulate cell  
319 proliferation in the adult mouse SVZ and that genetic silencing of GHSR does not decrease cell  
320 division in this niche.

321

322 **Acyl-ghrelin does not increase the number of new adult-born olfactory bulb neurones**

323 We recently showed that treatment with acyl-ghrelin increased adult hippocampal neurogenesis  
324 (AHN) in adult rats<sup>11</sup>. To determine whether acyl-ghrelin treatment modulates AOBN in a similar  
325 way to AHN, we quantified the number of new adult-born neurones in the OB of adult rats from  
326 the same study. Using OB tissue from the same rats whereby acyl-ghrelin increased AHN provides  
327 us with valuable experimental controls. We show there was no significant difference in the  
328 number of new adult-born cells (BrdU<sup>+</sup>/NeuN<sup>-</sup>) in the GCL of the OB following acyl-ghrelin  
329 treatment compared to saline treatment (figure 3G,  $P = 0.8482$ ). Similarly, no differences were  
330 observed in the number of new adult-born neurones (BrdU<sup>+</sup>/NeuN<sup>+</sup>) (figure 3H,  $P = 0.7388$ ) or in  
331 the rate of neurone differentiation (figure 3I,  $P = 0.6870$ ).

332

333 **Calorie restriction induces activation of new adult-born OB cells in a ghrelin-dependent**  
334 **manner**

335 To determine whether a CR-mediated increase in endogenous acyl-ghrelin was able to increase  
336 the expression of the proto-oncogene, c-Fos, in new adult-born OB cells, we analysed the number  
337 of active c-Fos<sup>+</sup> cells within the GCL, GL, SEZ and LOT in WT and ghrelin<sup>-/-</sup> mice. A two-way ANOVA  
338 revealed a statistically significant main effect of treatment on BrdU<sup>+</sup> ( $p=0.0031$ ) and BrdU<sup>+</sup>/c-Fos<sup>+</sup>  
339 ( $p=0.0487$ ) cells within the GCL. Comparatively, genotype and the interaction (treatment and  
340 genotype) showed a significant effect on c-Fos<sup>+</sup> ( $p=0.0001$  and  $0.017$ , respectively) and BrdU<sup>+</sup>/c-  
341 Fos<sup>+</sup> ( $p=0.0002$  and  $0.00021$ , respectively) cells within the GCL. Outside of the GCL, a significant  
342 main effect of treatment was reported in BrdU<sup>+</sup>/c-Fos<sup>+</sup> cells of the SEZ ( $p=0.0118$ ) and BrdU<sup>+</sup> cells  
343 of the LOT ( $p=0.0075$ ). No increase was observed within the GL (Table S1).

344 A Tukey post hoc test revealed a reduction in the number of new adult-born cells (BrdU<sup>+</sup>) in  
345 CR/re-fed (CR/RF) ghrelin<sup>-/-</sup> mice, compared with CR ghrelin<sup>-/-</sup> mice (figure 4C,  $P = 0.0086$ ) within  
346 the GCL. Furthermore, there was an increased number of activated cells (c-Fos<sup>+</sup>) in CR WT mice,  
347 compared with *ad libitum* WT ( $P = 0.0258$ ) and CR/RF WT ( $P = 0.0043$ ) mice. Notably, CR also  
348 increased activated cells in WT relative to CR ghrelin<sup>-/-</sup> mice ( $P < 0.0001$ ) within the GCL (figure  
349 4D). Further analysis revealed that the number of active new adult-born cells (BrdU<sup>+</sup>/c-Fos<sup>+</sup>) was  
350 increased in CR WT mice compared with CR/RF WT ( $P = 0.0169$ ) and CR ghrelin<sup>-/-</sup> mice  
351 ( $p < 0.0001$ ) within the GCL (figure 4E). Whereas, there were very few active developmentally  
352 born cells (BrdU<sup>+</sup>/c-Fos<sup>+</sup>) and these cells were not significantly affected by treatment or genotype  
353 (figure 4F). Outside of the GCL, the number of active new adult-born cells (BrdU<sup>+</sup>/c-Fos<sup>+</sup>) was  
354 reduced in CR ghrelin<sup>-/-</sup> mice, compared with *ad-libitum* fed ghrelin<sup>-/-</sup> mice ( $P = 0.0169$ ) within  
355 the SEZ. No significant differences were reported in the other regions tested (Table S1). There  
356 was no significant difference in body weight change in ghrelin<sup>-/-</sup> mice relative to WT mice in either  
357 of the groups (Two-way ANOVA; main effect of genotype,  $P = 0.9335$ ; main effect of feeding

358 pattern,  $P = 0.0049$ ; main effect of interaction (feeding pattern vs genotype),  $P = 0.3469$ ).  
359 Collectively, these data suggest that CR increases the activation of new adult-born cells in a  
360 ghrelin-dependent manner.

361

## 362 **Discussion**

363 The generation of new OB neurones in the adult brain is important for olfactory discrimination, a  
364 process that is impaired in ageing and several neurodegenerative disorders. Here, we tested the  
365 hypothesis that ghrelin is an important regulator of AOBN. First, we characterised expression of  
366 GHSR in the adult mouse brain. Numerous studies have attempted to characterise the expression  
367 pattern of GHSR in several species, including mouse, rat and lemur<sup>27-30</sup>, though the lack of reliable  
368 anti-GHSR antibodies have limited progress. More recently, a report using the GHSR-eGFP mouse  
369 and in situ hybridisation histochemistry demonstrated GHSR expression within the OB,  
370 hippocampus and hypothalamic nuclei<sup>15</sup>. Furthermore, Cre-activity in *Ghsr*-IRES-Cre/*ROSA26*-  
371 *ZsGreen* reporter mice was also reported in the main and accessory OB<sup>31</sup>.

372 Here, using adult GHSR-eGFP mice, we report GHSR immunoreactivity in the MCL, AON and  
373 orbital and motor orbital cortices of the OB, as well as within the anterior cingulate cortex, motor  
374 cortex, lateral septal nucleus, entopeduncular nucleus, hippocampus and the medial amygdaloid  
375 nucleus. However, GHSR was not expressed within the neurogenic niche of the SVZ in GHSR-eGFP  
376 reporter mice. Indeed, this finding is consistent with previous studies that do not report GHSR  
377 immunoreactivity within the SVZ niche. Together, these findings suggest that ghrelin does not  
378 mediate direct effects on NSPC proliferation.

379 As eGFP immunoreactivity in this transgenic model may correspond to two structurally different  
380 receptors, GHSR1a, which encodes the functional receptor, and the truncated GHSR1b, generated  
381 from alternative splicing of GHSR, we sought to identify GHSR1a expressing cells using antisera  
382 raised against GHSR1a. The specificity of polyclonal antibodies used to characterise GHSR within  
383 the adult brain remains unclear. Li *et al.*<sup>14</sup> reported GHSR expression within the adult mouse  
384 neurogenic niche of the SVZ using immuno-fluorescence with the rabbit anti-GHSR1a antibody  
385 (Phoenix Pharmaceuticals, H-001-62), diluted 1:500. In our study, using the same antibody, IHC  
386 in brain tissue from adult GHSR-null and WT mice revealed detectable immunoreactivity in tissue  
387 from both genotypes. Our data suggest that the rabbit anti-GHSR antibody resulted in non-specific  
388 staining within the SVZ and cingulate cortex (figure S1), preventing it's use to determine GHSR1a  
389 expression in this context. Combined, these studies suggest that the ghrelin receptor is not  
390 expressed in the SVZ, and thus does not directly modulate NSPC proliferation.

391 To determine whether ghrelin induces cell proliferation within the SVZ we treated GHSR-null and  
392 wild-type mice for 7-days with acyl-ghrelin. Subsequent analysis revealed no effect of genotype

393 or treatment on the number of dividing Ki67<sup>+</sup> cells in the SVZ. In contrast, a previous study  
394 reported that ghrelin<sup>-/-</sup> mice had a reduced number of proliferating NSPCs, migrating neuroblasts  
395 and OB interneurons, that could be restored to WT levels by intraperitoneal administration of  
396 acyl-ghrelin<sup>14</sup>. Several differences between the two experimental procedures might account for  
397 the contrasting results. For example, Li et al. used 8-9 week old WT and ghrelin<sup>-/-</sup> mice that  
398 received acyl-ghrelin (80 µg/kg) via intraperitoneal injection, once daily for 8 consecutive days.  
399 Whereas, in our study 14-week old WT and GHSR-null mice were given acyl-ghrelin (48 µg/day)  
400 via intravenous mini-pump. Therefore, inconsistencies between studies may be attributable to  
401 genetic background, the physiological dose or the route of administration of acyl-ghrelin.

402

403 Next, using a BrdU pulse-chase approach we determined the effect of exogenous acyl-ghrelin  
404 treatment on the maturation and survival of new adult-born neurones in the rat OB. Consistent  
405 with our previous cell proliferation analysis in mice, acyl-ghrelin did not increase in the number  
406 of new adult-born BrdU<sup>+</sup> cells or BrdU<sup>+</sup>/NeuN<sup>+</sup> neurones in the GCL of the OB. Furthermore, no  
407 differences were observed in the rate of neuronal differentiation. Notably, we have previously  
408 reported that adult hippocampal neurogenesis was significantly increased by acyl-ghrelin in  
409 these rats<sup>11</sup>. The high level of GHSR expression within hippocampal neurogenic niche<sup>12</sup> and it's  
410 absence in the SVZ niche is likely responsible for this effect. These data provide compelling  
411 evidence that acyl-ghrelin does not promote AOBN.

412 Numerous studies have suggested that ghrelin plays an important role in olfactory-related  
413 behaviours including odour discrimination and sensitivity<sup>8,32,33</sup>. Loch *et al.* reported an increased  
414 responsiveness of the mouse olfactory epithelium following nasal application of ghrelin. This  
415 resulted in a higher reactivity of olfactory sensory neurones within the olfactory epithelium,  
416 which in turn, increased the activity of receptor-specific glomeruli. GHSR expression on the  
417 surface of olfactory sensory neurones suggest that ghrelin and GHSR may play an important role  
418 in enhancing neuronal responsiveness and olfaction. However, the underlying mechanism by  
419 which acyl-ghrelin enhances olfaction remains elusive and it is unclear if new adult-born OB  
420 neurones are involved in this physiology.

421 As acyl-ghrelin is known to regulate both olfaction and appetite we sought to determine whether  
422 new adult-born OB neurones are activated by CR in a ghrelin-dependent manner. Our data  
423 demonstrate that overnight CR activated new adult-born cells in the OB. Re-feeding for one hour  
424 returned the number of c-Fos positive cells to baseline, suggesting that the new adult-born cells  
425 are sensitive to feeding status. Notably, this CR effect was absent in ghrelin<sup>-/-</sup> mice demonstrating  
426 that the activation of new adult-born cells was dependent upon intact ghrelin signalling.  
427 Furthermore, there was no CR-mediated activation of developmentally-born cells (BrdU<sup>-</sup>/c-Fos<sup>+</sup>)

428 in the GCL of the OB indicating that adult-born neurones are uniquely responsive to acute changes  
429 in food intake. Therefore, we confirm that CR activates new adult-born OB cells in a ghrelin-  
430 dependent manner. This finding provides further support for ghrelin acting as a mediator of CR-  
431 associated physiology, including, neuroprotection<sup>34</sup>, anti-anxiety<sup>35</sup>, hippocampal neurogenesis  
432 and cognitive enhancement<sup>12</sup>, and glycemic regulation<sup>36</sup>.

433 Although the relationship between hunger stimulation and olfaction has been long recognised, a  
434 molecular mechanism relating the two processes has not been determined<sup>37</sup>. Soria-Gomez *et al.*  
435 observed that cortical feedback projections to the OB crucially regulate food intake, possibly  
436 through cannabinoid type-1 receptor (CB1R) signalling. The endocannabinoid system, in  
437 particular CB-1Rs, promoted food intake in fasted mice by increasing odour detection. Notably,  
438 ghrelin's orexigenic effect is lost in CB-1R knock-out mice<sup>38</sup>. Although the relationship between  
439 ghrelin and the endocannabinoid system in the OB is unknown, both GHSR and CB-1R are GPCRs  
440 known to form homo- and heterodimers (or higher-order oligomers) as part of their normal  
441 trafficking and function<sup>39,40</sup>. Therefore, heterodimerisation of CB-1R and GHSR may be important  
442 in linking ghrelin to adult-born OB neurones and olfaction.

443 Several questions remain unanswered, including whether ghrelin alters the electrophysiological  
444 properties and/or directly activates GCs in the OB to enhance odour discrimination. As new adult-  
445 born OB cells enhance the odour-reward association<sup>3</sup>, further work is needed to determine  
446 whether the ghrelin-induced intake of rewarding foods<sup>41</sup> requires signalling via new neurones in  
447 the OB. Similarly, it is not known whether ghrelin can increase appetite and improve olfaction in  
448 the absence of new adult-born OB cells.

449 In summary, these data demonstrate that while ghrelin does not increase SVZ-OB neurogenesis,  
450 it does mediate the CR-induced activation of new adult-born OB cells. We speculate that ghrelin  
451 modulates new OB neurone activity to integrate olfactory responses with nutritional status.

452



453 **Figure legends**

454

455 **Figure 1. Characterisation of GHSR1a in the adult GHSR1a-eGFP mouse brain.**

456 (i). GHSR1a-eGFP immunoreactivity is present within the orbital and motor orbital cortex and the  
457 anterior olfactory nucleus. CTX, cortex; AON, anterior olfactory nucleus.

458 (ii). Collage of coronal mouse sections (A). Inset images of GHSR1a-eGFP immunoreactivity in  
459 anterior cingulate cortex dorsal (B), anterior cingulate cortex (C) and lateral septal nucleus (E).  
460 GHSR1a-eGFP immunoreactivity is absent in the lateral lining of the SVZ (D).

461 (iii). Collage of sagittal mouse sections (A). Inset images of GHSR1a-eGFP immunoreactivity in  
462 primary motor cortex (B), anterior amygdala area (D), dorsal granule cell layer of the dentate  
463 gyrus (E), ventral dentate gyrus (F) and medial amygdalar nucleus (posterodorsal)(G). GHSR1a-  
464 eGFP immunoreactivity is absent within the lateral lining of the SVZ (C).

465 Montage image scale bar = 200µm. Inset image scale bar = 50µm.

466

467 **Figure 2. Acyl-ghrelin treatment does not increase cell proliferation in the SVZ of adult**

468 **wild-type or GHSR-null mice.** (A) GHSR-null and WT littermate mice were treated for 7-days  
469 with either saline or acyl-ghrelin (48ug/day i.v) via osmotic mini-pump before brains were  
470 collected and Ki67 immunoreactivity quantified throughout the rostro-caudal extent of the SVZ.  
471 (B) Total number of Ki67+ cells did not change following acyl-ghrelin treatment in either WT or  
472 GHSR-null mice. Data are mean +/- SEM, n=3 mice per group. Statistical analysis performed by  
473 Kruskal-Wallis test ( $P = 0.2087$ ) followed by a post-hoc Dunn's multiple comparison test.

474

475 **Figure 3. Exogenous acyl-ghrelin does not increase the number of new adult born neurones**  
476 **in the granule cell layer of the rat olfactory bulb.** (A) Experimental paradigm. (B) Collage

477 image of the rat olfactory bulb. Representative images of BrdU (red) and NeuN (green) in (C)  
478 dorsal granule cell layer (GCL) and (D) ventral GCL of the OB. Scale bar = 200µm. Representative  
479 images of new adult-born neurones co-expressing NeuN+ and BrdU+ (yellow) in (E) dorsal GCL  
480 and (F) ventral GCL. Scale bar = 50µm. Quantification of new adult-born OB cells (G) ( $P = 0.8482$ ),  
481 new adult-born neurones (H) ( $P = 0.7388$ ) and % neuronal differentiation (I) ( $P = 0.6870$ ) after  
482 acyl-ghrelin or saline treatment. Data are mean +/- SEM. Statistical analysis was performed by  
483 two-tailed unpaired Student's *t*-test.  $P < 0.05$  considered significant, ns = not significant. n = 11  
484 rats per group.

485

486 **Figure 4. New adult-born OB cells are activated by calorie restriction in a ghrelin-**  
487 **dependent manner.** (A) Schematic of experimental paradigm. (B) New adult-born active

488 neurone (yellow; scale bar = 25µm) co expressing BrdU (green) and c-Fos (red) in the GCL of the  
489 OB. Scale bar = 50µm. Quantification of (C) new adult-born cells (BrdU<sup>+</sup>), (D) active cells (c-Fos<sup>+</sup>),  
490 (E) active new adult-born cells (BrdU<sup>+</sup>/c-Fos<sup>+</sup>) and (F) active developmentally born cells (BrdU<sup>-</sup>/  
491 /c-Fos<sup>+</sup>) in the GCL of the OB. (G) Representative images of new adult-born cells (BrdU<sup>+</sup>; green),  
492 active cells (c-Fos<sup>+</sup>; red) and active new adult-born cells (BrdU<sup>+</sup>/CFos<sup>+</sup>; yellow in merged image).  
493 Arrows correspond to new BrdU<sup>+</sup>/c-Fos<sup>-</sup> cells, whilst arrowheads represent active new adult-  
494 born BrdU<sup>+</sup>/c-Fos<sup>+</sup> cells. Scale bar = 50µm. Statistical analysis was performed by two-way ANOVA  
495 with Tukey post hoc test. \* P ≤ 0.05, \*\* P ≤ 0.01, \*\*\*\* P ≤ 0.0001. All data shown are mean +/-SEM;  
496 n = 5-8 rats per group. AL (ad-libitum), CR (calorie restriction), CR/RF (calorie restriction / re-  
497 fed), WT (wild-type), GKO (ghrelin<sup>-/-</sup>).  
498

499 **References**

- 500 1. Lledo, P.-M., Alonso, M. & Grubb, M. S. Adult neurogenesis and functional plasticity in  
501 neuronal circuits. *Nat. Rev. Neurosci.* **7**, 179–93 (2006).
- 502 2. Alonso, M. *et al.* Activation of adult-born neurons facilitates learning and memory. *Nat.*  
503 *Neurosci.* (2012). doi:10.1038/nn.3108
- 504 3. Grelat, A. *et al.* Adult-born neurons boost odor–reward association. *Proc. Natl. Acad. Sci.*  
505 201716400 (2018). doi:10.1073/pnas.1716400115
- 506 4. Imayoshi, I. *et al.* Roles of continuous neurogenesis in the structural and functional  
507 integrity of the adult forebrain. **11**, 1153–1161 (2008).
- 508 5. Mesholam, R. I., Moberg, P. J., Mahr, R. N. & Doty, R. L. Olfaction in Neurodegenerative  
509 Disease. *Arch. Neurol.* **55**, 84 (1998).
- 510 6. Boesveldt, S. *et al.* A comparative study of odor identification and odor discrimination  
511 deficits in Parkinson’s disease. *Mov. Disord.* **23**, 1984–1990 (2008).
- 512 7. Andrews, Z. B. The extra-hypothalamic actions of ghrelin on neuronal function. *Trends*  
513 *Neurosci.* **34**, 31–40 (2011).
- 514 8. Tong, J. *et al.* Ghrelin Enhances Olfactory Sensitivity and Exploratory Sniffing in Rodents  
515 and Humans. *J. Neurosci.* **31**, 5841 LP-5846 (2011).
- 516 9. Malik, S., McGlone, F., Bedrossian, D. & Dagher, A. Ghrelin Modulates Brain Activity in  
517 Areas that Control Appetitive Behavior. *Cell Metab.* **7**, 400–409 (2008).
- 518 10. Zhao, Z. *et al.* Ghrelin administration enhances neurogenesis but impairs spatial learning  
519 and memory in adult mice. *Neuroscience* **257**, 175–85 (2014).
- 520 11. Kent, B. A. *et al.* The orexigenic hormone acyl-ghrelin increases adult hippocampal  
521 neurogenesis and enhances pattern separation. *Psychoneuroendocrinology* **51**, 431–439  
522 (2015).
- 523 12. Hornsby, A. K. E. *et al.* Short-term calorie restriction enhances adult hippocampal  
524 neurogenesis and remote fear memory in a Ghnr-dependent manner.  
525 *Psychoneuroendocrinology* **63**, 198–207 (2016).
- 526 13. Walker, a K. *et al.* The P7C3 class of neuroprotective compounds exerts antidepressant  
527 efficacy in mice by increasing hippocampal neurogenesis. *Mol. Psychiatry* 1–9 (2014).  
528 doi:10.1038/mp.2014.34
- 529 14. Li, E. *et al.* Ghrelin stimulates proliferation, migration and differentiation of neural  
530 progenitors from the subventricular zone in the adult mice. *Exp. Neurol.* **252**, 75–84  
531 (2014).
- 532 15. Mani, B. K. *et al.* Neuroanatomical characterization of a growth hormone secretagogue  
533 receptor-green fluorescent protein reporter mouse. *J. Comp. Neurol.* **3666**, 3644–3666  
534 (2014).

- 535 16. Goetzl, F. & Stone, F. Diurnal variations in acuity of olfaction and food intake.  
536 *Gastroenterology* **9**, 444–453 (1947).
- 537 17. Aimé, P. *et al.* Fasting increases and satiation decreases olfactory detection for a neutral  
538 odor in rats. *Behav. Brain Res.* **179**, 258–264 (2007).
- 539 18. Reichenbach, A., Steyn, F. J., Sleeman, M. W. & Andrews, Z. B. Ghrelin receptor expression  
540 and colocalization with anterior pituitary hormones using a GHSR-GFP mouse line.  
541 *Endocrinology* **153**, 5452–5466 (2012).
- 542 19. Zigman, J. M. *et al.* Mice lacking ghrelin receptors resist the development of diet-induced  
543 obesity. *J. Clin. Invest.* **115**, 3564–3572 (2005).
- 544 20. Davies, J. S. *et al.* Ghrelin induces abdominal obesity via GHS-R-dependent lipid retention.  
545 *Mol. Endocrinol.* **23**, 914–24 (2009).
- 546 21. Sun, Y., Ahmed, S. & Smith, R. G. Deletion of ghrelin impairs neither growth nor appetite.  
547 *Mol. Cell. Biol.* **23**, 7973–7981 (2003).
- 548 22. Wortley, K. E. *et al.* Genetic deletion of ghrelin does not decrease food intake but  
549 influences metabolic fuel preference. *Proc. Natl. Acad. Sci.* **101**, 8227–8232 (2004).
- 550 23. McFarlane, M. R., Brown, M. S., Goldstein, J. L. & Zhao, T. J. Induced ablation of ghrelin cells  
551 in adult mice does not decrease food intake, body weight, or response to high-fat diet. *Cell*  
552 *Metab.* **20**, 54–60 (2014).
- 553 24. Zhang, W., Hu, Y., Lin, T. R., Fan, Y. & Mulholland, M. W. Stimulation of neurogenesis in rat  
554 nucleus of the solitary tract by ghrelin. **26**, 2280–2288 (2005).
- 555 25. Zhang, W. *et al.* Ghrelin stimulates neurogenesis in the dorsal motor nucleus of the vagus.  
556 **3**, 729–737 (2004).
- 557 26. Moon, M., Hwang, L. & Park, S. Ghrelin Regulates Hippocampal Neurogenesis in Adult  
558 Mice. *Endocr. J.* **56**, 525–531 (2009).
- 559 27. Guan, X. *et al.* Distribution of mRNA encoding the growth hormone secretagogue receptor  
560 in brain and peripheral tissues. *Mol. Brain Res.* **48**, 23–29 (1997).
- 561 28. Mitchell, V. *et al.* Comparative distribution of mRNA encoding the growth hormone  
562 secretagogue-receptor (GHS-R) in *Microcebus murinus* (Primate, Lemurian) and rat  
563 forebrain and pituitary. *J. Comp. Neurol.* **429**, 469–489 (2000).
- 564 29. Sun, Y., Garcia, J. M. & Smith, R. G. Ghrelin and Growth Hormone Secretagogue Receptor  
565 Expression in Mice during Aging. *Endocrinology* **148**, 1323–1329 (2007).
- 566 30. Zigman, J. M., Jones, J. E., Lee, C. E., Saper, C. B. & Elmquist, J. K. Expression of ghrelin  
567 receptor mRNA in the rat and the mouse brain. *J. Comp. Neurol.* **494**, 528–548 (2006).
- 568 31. Mani, B. K. *et al.* The role of ghrelin-responsive mediobasal hypothalamic neurons in  
569 mediating feeding responses to fasting. *Mol. Metab.* **6**, 882–896 (2017).
- 570 32. Loch, D., Breer, H. & Strotmann, J. Endocrine Modulation of Olfactory Responsiveness:

571 Effects of the Orexigenic Hormone Ghrelin. *Chem. Senses* **40**, 469–479 (2015).

572 33. Prud'homme, M. J. *et al.* Nutritional status modulates behavioural and olfactory bulb Fos  
573 responses to isoamyl acetate or food odour in rats: roles of orexins and leptin.  
574 *Neuroscience* **162**, 1287–1298 (2009).

575 34. Bayliss, J. *et al.* Ghrelin-AMPK signalling mediates the neuroprotective effects of Calorie  
576 Restriction in Parkinson's Disease. *J. Neurosci.* **36**, 3049–3063 (2016).

577 35. Lutter, M. *et al.* The orexigenic hormone ghrelin defends against depressive symptoms of  
578 chronic stress. *Nat. Neurosci.* **11**, 10–11 (2008).

579 36. Zhao, T.-J. *et al.* Ghrelin O-acyltransferase (GOAT) is essential for growth hormone-  
580 mediated survival of calorie-restricted mice. *Proc. Natl. Acad. Sci. U. S. A.* **107**, 7467–72  
581 (2010).

582 37. Soria-Gómez, E. *et al.* The endocannabinoid system controls food intake via olfactory  
583 processes. *Nat. Neurosci.* (2014). doi:10.1038/nn.3647

584 38. Kola, B. *et al.* The orexigenic effect of ghrelin is mediated through central activation of the  
585 endogenous cannabinoid system. *PLoS One* **3**, e1797 (2008).

586 39. Prinster, S. C., Hague, C. & Hall, R. A. Heterodimerization of G Protein-Coupled Receptors :  
587 Specificity and Functional Significance. **57**, 289–298 (2005).

588 40. Wellman, M. & Abizaid, A. Growth Hormone Secretagogue Receptor Dimers: A New  
589 Pharmacological Target. *eneuro* (2015).

590 41. Egecioglu, E. *et al.* Ghrelin increases intake of rewarding food in rodents. *Addict. Biol.* **15**,  
591 304–311 (2010).

592

593

Figure 1. Ratcliff *et al.*

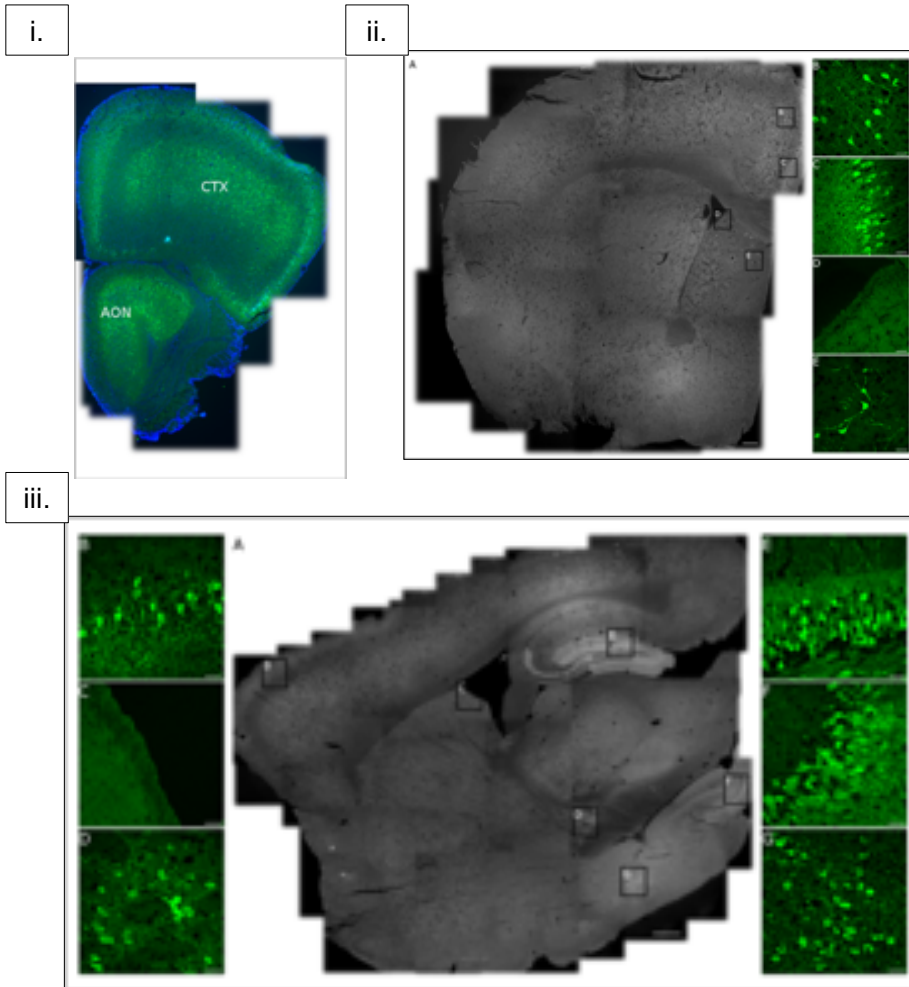


Figure 2. Ratcliff *et al.*

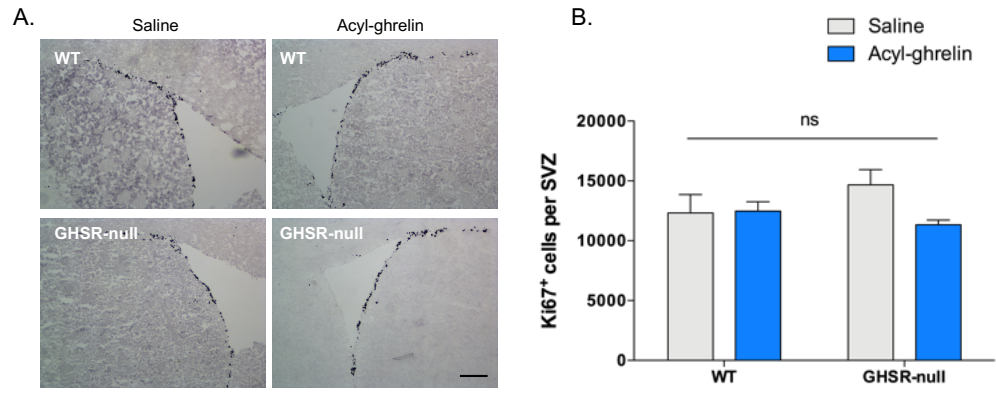


Figure 3. Ratcliff *et al.*

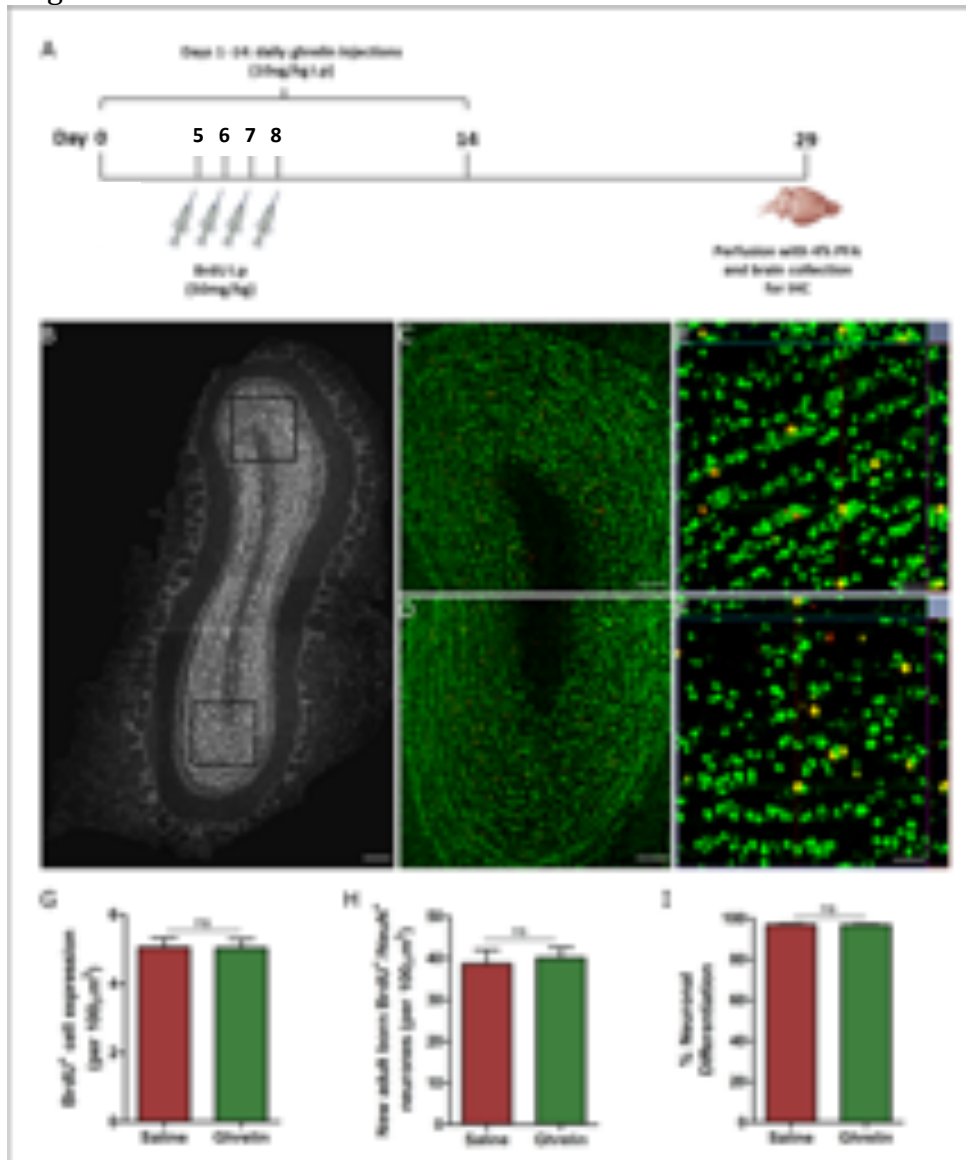
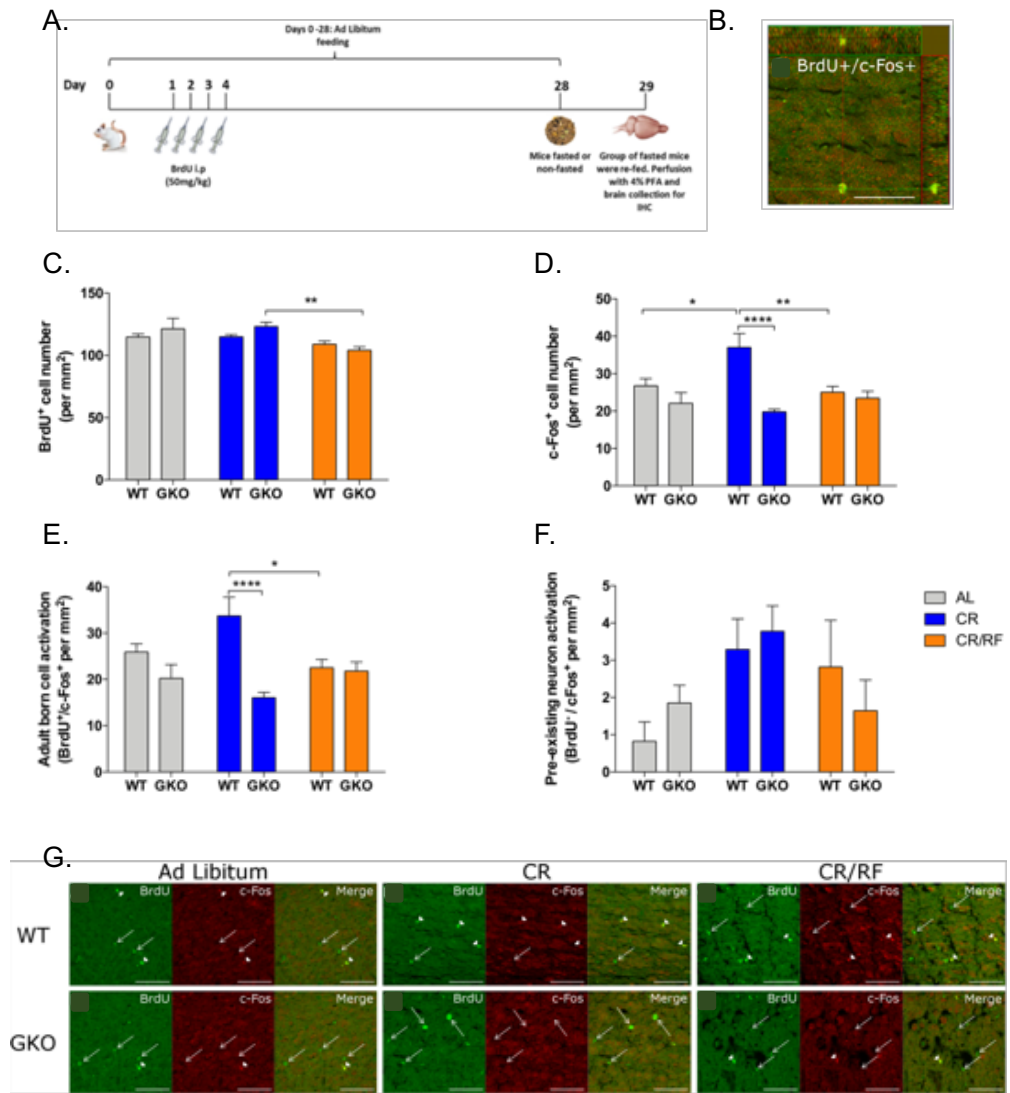


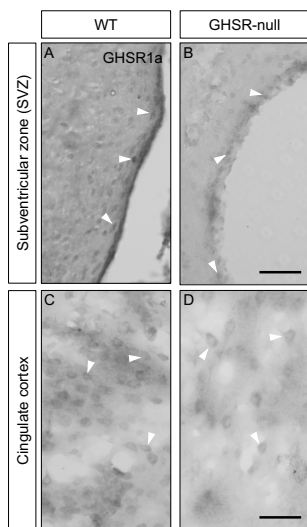


Figure 4. Ratcliff *et al.*



597

598



**Figure S1.** Immunoreactivity (IR, white arrowheads) for anti-GHSR1a was observed in the adult SVZ of both WT (A) and GHSR-null (B) mice. Similar IR was observed in the cingulate cortex of WT (C) and GHSR-null (D) mice. These data suggest that the rabbit anti-GHSR1a antisera cross-reacted with nonspecific antigen in the adult mouse brain. Scale bar = 50 $\mu$ m.

601 Table S1. Ratcliff *et al.*

Region	Cellular expression	Statistical Significance (P-value)		
		Interaction (treatment - genotype)	Treatment	Genotype
GCL	BrdU <sup>+</sup>	0.1753	0.0031 **	0.2941
	c-Fos <sup>+</sup>	0.017 *	0.0955	0.0001 ****
	BrdU <sup>+</sup> /c-Fos <sup>+</sup>	0.0021 **	0.4737	0.0002 ***
	BrdU <sup>-</sup> /c-Fos <sup>+</sup>	0.42	0.0487 *	0.8718
GL	BrdU <sup>+</sup>	0.316	0.7846	0.9092
	c-Fos <sup>+</sup>	0.5313	0.6372	0.9362
	BrdU <sup>+</sup> /c-Fos <sup>+</sup>	0.2824	0.9716	0.6254
	BrdU <sup>-</sup> /c-Fos <sup>+</sup>	0.532	0.2843	0.0868
SEZ	BrdU <sup>+</sup>	0.6798	0.2156	0.9714
	c-Fos <sup>+</sup>	0.844	0.2227	0.1342
	BrdU <sup>+</sup> /c-Fos <sup>+</sup>	0.2951	0.0118 *	0.573
	BrdU <sup>-</sup> /c-Fos <sup>+</sup>	0.8253	0.074	0.3409
AOL	BrdU <sup>+</sup>	0.5858	0.0075 **	0.9319
	c-Fos <sup>+</sup>	0.6191	0.6312	0.5688
	BrdU <sup>+</sup> /c-Fos <sup>+</sup>	No colocalisation (p=1.0000)		
	BrdU <sup>-</sup> /c-Fos <sup>+</sup>	0.4821	0.1376	0.4439

**Table S1. New adult-born OB cells are activated by calorie restriction in a ghrelin-dependent manner.** Main effects of two-way ANOVA. \*p<0.05; \*\*p<0.01; \*\*\*p<0.001; \*\*\*\*p<0.0001 were considered statistically significant. GCL (granule cell layer), GL (glomerular layer), SEZ (subependymal zone), AOL (anterior olfactory nucleus, lateral).